Misclassification error rejection in structural models for spatial architectures

Structures 67 (2024) 106997

Contents lists available at ScienceDirect

Structures

journal homepage: www.elsevier.com/locate/structures

Misclassification error rejection in structural models for spatial architectures

Gaetano Miraglia [a,b,*,1], Erica Lenticchia [a,b,2], Linda Scussolini [a,3], Rosario Ceravolo [a,b,4]

[a] Department of Structural, Building and Geotechnical Engineering, Politecnico di Torino, Corso Duca degli Abruzzi 24, 10129 Turin, Italy
[b] Responsible Risk Resilience interdepartmental Centre (R3C), Politecnico di Torino, Corso Duca degli Abruzzi 24, 10129, Turin, Italy

ARTICLE INFO

Keywords:
Experimental campaigns
Gaussian mixture models
Hilbert-Huang Transform
Natural frequency
Sensitivity analysis
Spatial architectures
Vibration mode coupling
Vibration mode pairing

ABSTRACT

Vibration mode pairing via modal coupling and modal assurance criteria is a task encountered in different applications of Structural Health Monitoring. Above these, Sensitivity Analysis, and Model Updating need a correct estimation of the pairing between a reference set of vibration modes (that can be both numerical or experimental) and different sets of numerical vibration modes, generated by the variations of structural model parameters. The incorrect pairing, or coupling, results in error propagation during the sensitivity analysis or model updating, generating biased results. In this paper, the authors propose a reliable and efficient method to reduce the effects of mode pairing (i.e., mode coupling) errors in the calculation of the sensitivity of modal data to mechanical parameter variations, even under complex conditions such as complex numerical models of spatial structures, where the vibration modes are characterized by, for example, high-order mode shapes and high probability of confusing correlated mode shapes. The proposed method is based on the conjunction application of Hilbert-Huang Transform to remove outliers, and Gaussian Mixture Models to alleviate the elimination of meaningful information during the outliers rejection phase. In particular, knowing the actual sensitivity of the vibration modes not only allows to optimize the subsequent automatic model updating phase, but even before that, it allows to optimize the design of a permanent monitoring system, for example by predicting the direction and position of the sensors which maximize the extractable modal information considering that the mechanical parameters are continuously subjected to Environmental and Operational Variations, or again, would allow the optimization of extended experimental campaigns, suggesting additional number of mechanical tests for those structural components which most influence the modal behavior of the structure.

1. Introduction

During the process of knowledge of the structural behavior of physical systems, an important task is to identify the causes and quantify the effects of variation of its mechanical parameters. This task cannot be performed on the actual structure since it would consist of drastically varying its structural characteristics. However, a virtual model can be designed for this purpose.

As a part of this process, a sensitivity analysis activity [1,2] is aimed at evaluating the effect that the variation of a single mechanical parameter of a numerical model produces on another parameter of the same model (e.g., modal parameters, such as natural frequency). The first step in carrying out this type of activity is data collection, a task that can also be useful for future condition assessment and monitoring analyses [3]. In this step, the numerical model is interrogated to generate data on the vibration modes of the system, such as the values assumed by the mechanical parameters. The problem with applying this procedure with modal data is that the individual vibration modes are ordered in the numerical model in a non-predefined order, which varies with the variation of the value assumed by the mechanical parameter. In other words, to perform a sensitivity analysis of modal data, it is necessary to implement a *mode pairing* or *mode coupling* (also known as *mode tracking*

* Correspondence to: Corso Duca degli Abruzzi 24, 10129, Torino, Italy.
E-mail address: gaetano.miraglia@polito.it (G. Miraglia).
[1] [0000–0002-3611–0215]
[2] [0000–0002-3746–2933]
[3] [0000–0001-7883–111X]
[4] [0000–0001-5880–8457]

https://doi.org/10.1016/j.istruc.2024.106997
Received 21 December 2023; Received in revised form 10 June 2024; Accepted 24 July 2024
Available online 1 August 2024

when the time is the independent variable of the problem) procedure [4–7]. To achieve this, a reference model, characterized by a set of mechanical reference parameters, is used to generate the reference modal data, which will be used as a comparison term during the sensitivity analysis. This reference model must consider the information gathered experimentally as much as possible, for example through in-situ mechanical tests, which play a fundamental role in estimating an accurate sensitivity indicator. To evaluate the coupling between the single reference mode and a set of vibrating modes extracted from a model (to which a different set of tentative mechanical parameters has been attributed), it is possible to use the Modal Assurance Criterion (MAC) [8,9] or alternative techniques aimed at comparing two different vibration modes for different aims, such as damage identification [10]. The closer the MAC is to one, the more the single extracted mode will be correlated to the reference mode. The vibration mode coupled to the reference mode will have the highest MAC value among those extracted. This procedure allows the tracking of the various reference vibration modes, obtaining, as the mechanical parameters vary, how the order of the mode varies within the mechanical model.

The problem with this procedure is that the vibration modes with a high MAC can sometimes be misinterpreted because of minor process errors (e.g., the mesh discretization of the numerical model) affect the MAC estimation. In this context, the *correct* mode to be coupled to the reference one is characterized by a lower MAC value than the mode with the highest MAC.

To alleviate this problem, the mode pairing strategies improved indicators to investigate the correlation between (mostly) an experimentally identified modal vector and the respective mode shape of a numerical model, being the correlation always possible even between experimental and experimental vibration modes (mode tracking), and between numerical and numerical vibration modes (i.e., mode coupling or pairing). Some of these indicators are described in standard textbooks on experimental and operational modal analysis [11–13]. About these, one can find for example [4]:

Modal Scale Factor (MSF) [14]: it is one of the first measures for the correlation of two mode shapes and was originally developed to assist in modal analysis. The MSF is a non-normalized indicator dependent on the scaling of two vectors, thus the magnitude of MSF is heavily influenced by the normalization applied during analysis. This can pose challenges in correctly assigning respective modes, especially when different normalizations are used.

Modal Assurance Criterion (MAC) [14,15]: it is the most widely used method to check the correlation between experimental and numerical modal vectors. MAC does not require coordinate-complete experimental eigenvectors or system matrices. It is independent of the scaling of mode shapes, making it a robust indicator. The MAC value ranges from zero to one, with values closer to one indicating a higher linear dependency.

Normalized Modal Differences (NMD) [12]: related to both MAC and MSF, NMD indicator suggests maximal correlation by a value of zero. Unlike MAC, NMD is unbounded and can yield values up to infinity in the case of perfect orthogonal mode shapes, which can be a practical drawback.

Linear Modal Assurance Criterion (LMAC) [16]: the LMAC was developed to address some limitations of MAC. LMAC linearizes the nonlinear behavior of MAC, resulting in higher sensitivity for nearly identical modal vectors. This increased sensitivity makes LMAC particularly useful in distinguishing similar modes.

Coordinate Modal Assurance Criterion (COMAC) and Enhanced COMAC (ECOMAC) [17,18]: both COMAC and its extension ECOMAC emphasize the discrepancy of specific degrees of freedom, requiring preliminary mode pairing. These criteria provide a detailed local assessment of mode shapes, which is especially valuable in structural health monitoring and damage detection, but not really useful in mode coupling.

Normalized Cross Orthogonality (NCO) [13,16]: the NCO, also known as Weighted Modal Assurance Criterion, incorporates additional physical information of the structure by using reduced or expanded mass or stiffness matrices from numerical models. This criterion offers certain advantages over MAC, such as integrating detailed structural information. However, the necessary reduction or expansion procedures can introduce additional errors and inaccuracies.

For further literature on the problem the readers can refer to [4–6].

Although correlation indicators are indispensable tools in vibration mode pairing as they provide a quantitative means to assess the relationship between vibration modes, they tend to fail under certain conditions [4], such as for example in presence of low-resolution numerical models, or numerical models of structures characterized by a high number of correlated vibrating modes (e.g., this is the case of spatial structures). For these reasons, instead to try to propose a new correlation indicator for paring vibration modes, in this paper the author propose a method to reduce the errors produced by a not correct coupling (i.e., misclassification errors) avoiding their propagation in subsequent activities, such as sensitivity analysis.

The method proposed in this paper mitigates this misclassification problem, regardless of the indicator used, through the combined use of: (i) Analogies with time-frequency analysis of the generated data, and (ii) Gaussian Mixture (GM) model fitted to data. Section 2 reports the proposed method to alleviate the misclassification error in mode tracking/coupling for sensitivity analysis. Section 3 describes the reference benchmark system, i.e., Morandi's iconic structure of the Pavilion V of the Turin Exhibition Center. In Section 4 the methods are applied to the benchmark structure, and the results of the analysis are critically discussed. Finally, conclusions of the study are drawn in Section 5.

1.1. Research significance

The problem that this work want to put in light is that the series of natural frequency and MAC values defined as function of mechanical parameter values of a numerical model are not autocorrelated. Thus, for each value of a selected parameter p_j, a set of vibration modes is extracted without correlation with the subsequent set associated to a new sampled value of p_j. In this situation, the calculation of the variance (or in general, a variation metric) of the natural frequency cannot be performed, because the classes of vibration modes do not exist. To generate classes of vibration modes that contain correlated quantities, a mode coupling analysis should be performed [19]. However, this task always foresees the possibility of errors that can contaminate subsequent structural analyses, such as sensitivity analysis. The main objective of the paper is thus to reduce these errors in the calculation of the sensitivity. In the paper the authors propose to idealize the historical series of natural frequency and MAC obtained after the coupling analysis such as time-history data, and to apply time-frequency and statistical methods of outliers rejection for the rejection of errors that can arise while trying to pair the vibration modes between the different sets. Solving this problem is quite important for real applications, such as for example the correct design of extensive and permanent dynamic sensing systems. In particular, coupling errors can falsely increase the sensitivity of a structural parameter (and thus a structural component) to the variation of specific vibration modes, guiding the path of knowledge toward incorrect structural elements, causing the available monetary resources to be wasted. Eliminating errors in the sensitivity calculation, in addition to guaranteeing less waste of monetary resources, guarantees an optimized design of the dynamic monitoring system [20], and the money saved thanks to a correct optimization can be channeled to guarantee greater structural knowledge of the structure to be to monitored.

2. Method

By interrogating the virtual model, it is possible to define the historical series of the natural frequency of a specific reference vibration mode k, $f_k(p_j)$ and $MAC_k(p_j)$, as a function of the value assumed by the j-

th mechanical parameter p_j, which represents the independent variable of the problem and regulates the natural frequency and MAC variation. In line with the concept of *local* sensitivity analysis, this can be repeated for each mechanical parameter j of the model and for each assumed reference mode k. The uncorrelated set of modal data are then correlated during the coupling analysis, for example, by comparing the MAC value of the vibration modes estimated in different sets. Autocorrelated historical series of natural frequency are thus obtained, which can contain errors, or outliers, due to the coupling analysis. To alleviate this problem the authors proposes to analyze the historical series of natural frequency with methods of outlier rejection used on time series, such as time-frequency analysis [21] or probabilistic methods, and then to calculate the sensitivity [22] on the historical series of natural frequency after the application of the outliers rejection task. In time-frequency methods, for example, the Hilbert-Huang Transform (HHT) has been successfully used for outliers rejection [23], while a common probabilistic method used for this aim is represented by the 3-σ rule [24]. In this work, time-frequency methods are used to reduce coupling errors that can contaminate the sensitivity estimates, while probabilistic methods are used to reduce the effect of eliminating meaningful information during the rejection of outliers.

The methods are then applied to a numerical model of a structure, whose mechanical parameters are initialized based on *una tantum* tests. The results provide a clear configuration of what structural element should be deeply investigated to optimize the design of future dynamic permanent sensing systems, or to perform future activities of automatic model updating based on modal data.

2.1. Time-frequency analogy

The MAC data, which represents the complement to one of the coupling errors $o_k(p_j)$, can be analyzed with signal analysis techniques belonging to time-frequency methods [25–27], assuming the considered mechanical parameter as an independent variable instead of time. These are techniques that simultaneously provide localized information in time and frequency domains through the estimate of Time-Frequency Distributions (TFD) (see, for example, [28] for well-established reference notations). The use of these distributions is fundamental in the study of non-stationary signals, for which the frequency distribution of the energy or power of the signal does not remain constant over time. There are plenty of TFDs that can be used for different purposes, even if they were initially conceptualized for describing the true nature of a signal and exploiting the joint information to infer behaviors and, at first sight, unknown phenomena [28]. For example, they can be used to [29]: (i) instantaneous natural frequency estimation of time-varying systems; (ii) mechanical parameter identification of time-varying structures; (iii) structural damage detection; (iv) nonlinear structural modeling, verification, and validation; (v) model selection for nonlinear structures; etc.

In this work, the TFD will be used to detect *anomalies* in signals behavior. For its sparse nature (convenient for the present study), the HHT will be assumed as TFD [30]. The modal datum is decomposed by Empirical Mode Decomposition (EMD) [10,31]. The result of the decomposition is a series of Intrinsic Mode Functions (IMFs) c and a residual signal (i.e., trend) r, the sum of which provides the starting signal. The EMD of a generic sample of signal s_i, with i indicator of the sample of the signal s, is defined as:

$$\boldsymbol{s_i} = \sum_{z=1}^{Z} \boldsymbol{c_{z,i}} + \boldsymbol{r_i} \tag{1}$$

where in Eq. (1), Z indicates the number of IMFs, while z denotes the generic IMF. The IMFs are basically quantities that respect two hypotheses:

- the upper and lower envelopes are symmetric;
- the number of zero-crossings and the number of extrema are exactly equal, or they differ by one at most.

The IMFs, estimated recurring the *sifting* algorithm [32], are used for the estimation of the HHT [33], [34], and in particular for the estimate of its power spectrum. The HHT is constructed starting from the analytic signals of the IMFs:

$$\boldsymbol{c_z} + \boldsymbol{jH}(\boldsymbol{c_z}) \tag{2}$$

where in Eq. (2), j indicates the imaginary part while $H(\bullet)$ denotes the Hilbert transform operator. The analytic form of the continuous signal $s(x)$, with x generic independent variable, becomes:

$$\boldsymbol{S}(\boldsymbol{x}) = \sum_{z=1}^{Z} \boldsymbol{a_z}(\boldsymbol{x}) \bullet \boldsymbol{e}^{j\vartheta_z(x)} \tag{3}$$

where in Eq. (3), a_z and ϑ_z, are the instantaneous amplitude and phase of the signal, while $\partial\vartheta_z(x)/\partial x$ denotes the *z-th* instantaneous frequency. The analogy of this work resides in assuming $x = p_j$ and $s = f_k$, $s = o_k$, or $s = MAC_k$. Thus, based on the type of signal assumed, the time is replaced with the input parameter value of the sensitivity analysis, while the frequency axis is replaced by the rate l (symbolically l=1/p) of the parameter. The peculiarity of the HHT spectrum is that it provides a sparse representation of the signal in the joint parameter / parameter-rate domain. Thus, the misclassification errors are easily detectable as high-rate components in the Hilbert-Huang domain (since it is assumed that the signals analyzed have smooth behavior, and abrupt change where errors occur). By assuming a threshold value of the parameter-rate (calibrated on observations), it is possible to reject the values of the parameters referred to as the non-zero values of the power spectrum, above the threshold. Rejecting these parameter values also means rejecting the associated natural frequency values, or, in other words: it is possible to correct the variation of the modal data by rejecting the variation component due to the misclassification error.

2.2. Gaussian mixture models

Since some of the modal data values are discarded from the calculation of sensitivity indicators used to estimate the amount of variation, it may occur that the dataset constituted by natural frequency is split into two or more classes virtually divided by "empty space" generated by the rejection of the parameters and natural frequencies associated with power spectrum of MAC having values, at parameter-rate above threshold, different from zero in the Hilbert-Huang space. This leads to a problem in estimating the variation of the modal datum (i.e., natural frequency), as the statistical distribution associated with it could be characterized by several modes (i.e., more components of a multivariate Probability Density Function, PDF). In this situation, the variation to be estimated is not that of the entire PDF (which, in fact, would mean re-introducing a variation component generated by the misclassification error) but rather a combination of the variations due to the single components of the multivariate distribution. In the present work, in order to estimate the *variance* and the *mean* of the different components of the multivariate distribution, a naive solution has been adopted by assuming the gaussianity of each component. In this way, it is possible to use the iterative Expectation-Maximization (EM) algorithm to fit a GM model on natural frequency data [35], [36], already cleaned by the misclassification errors:

$$\boldsymbol{g_V}(\boldsymbol{y}|\boldsymbol{\mu_v}, \boldsymbol{\Sigma_v}, \boldsymbol{w_v}) = \sum_{v=1}^{V} \boldsymbol{w_v}(2\pi)^{-\frac{d}{2}}|\boldsymbol{\Sigma_v}|^{-\frac{1}{2}} exp\left(-\frac{1}{2}(\boldsymbol{y}-\boldsymbol{\mu_v})^{\mathrm{T}}\boldsymbol{\Sigma_v^{-1}}(\boldsymbol{y}-\boldsymbol{\mu_v})\right) \tag{4}$$

where in Eq. (4), g_V is the GM PDF of order V, $\boldsymbol{y}$ is a multidimensional natural frequency vector $\mathbb{R}^{dx1}$, v denotes the component, while $\boldsymbol{\mu_v}$, $\boldsymbol{\Sigma_v}$ and w_v are the mean vector $\mathbb{R}^{dx1}$, covariance matrix $\mathbb{R}^{dxd}$, and

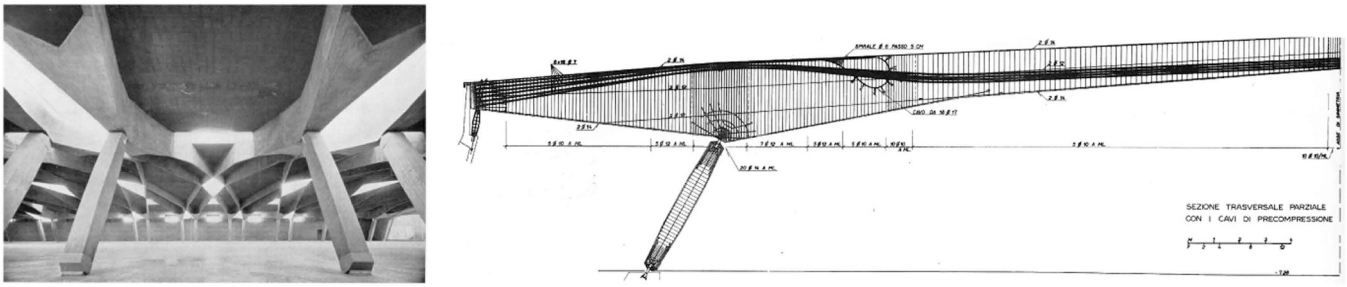

Fig. 1. Interior view of the Morandi's Pavilion V after its construction (on the left), section of the main element of the structure, the strut elements and the post-tensioned beam (on the right).

component proportion $\mathbb{R}^{1\times1}$ respectively. In this study, since a local sensitivity analysis is pursued, the dimension d equals one. For each component, the mean and covariance values that maximized the likelihood of the PDF can thus be obtained.

2.3. Mahalanobis distance

It should be noted that not all classes of natural frequency are associated with a *correct coupling* with the reference mode. Correct coupling means that a generic vibration mode is correctly paired to a specific reference vibration mode, independently by the indicator used to evaluate the goodness of the pairing. This can be easily done by visually checking at posteriori the mode shapes (after the model coupling procedure) or relying, when possible, to the MAC evaluated over the all Degrees of Freedom (DoFs) of an highly refined Finite Element (FE) model, after the coupling procedure (even if this operation is quite computational consuming in terms of vibrational mode extraction, and it is unfeasible to perform in reasonable time during the mode coupling analysis if a high-fidelity simulator is investigated).

The error in coupling happens because in the data sampling phase (i.e., simulation of the Operational Modal Analysis - OMA experiment [37,38]) it can happen to collect a series of uniform values referred to mechanical parameters which do not produce vibration modes comparable with the reference vibration mode at all. In this situation, it is understandable that natural frequency values close to the reference value are certainly more reliable than those far from them. Consequently, in this work, it was assumed to estimate the variation of the modal datum as that referred to the component of the GM model having the minimum distance from the reference datum. The Mahalanobis Distance (MD) [39] δ_v was used to estimate the distance between the reference datum (a point) and the component v of the GM model (a distribution):

$$\boldsymbol{\delta_v} = \sqrt{(\boldsymbol{y}-\widehat{\boldsymbol{\mu}}_v)^{\mathrm{T}}\widehat{\boldsymbol{\Sigma}}_v^{-1}(\boldsymbol{y}-\widehat{\boldsymbol{\mu}}_v)} \tag{5}$$

where in Eq. (5), $\widehat{(\bullet)}$ means estimated quantity.

2.4. Normalized variation

A procedure of this type can lead to an underestimation of the variation of the modal data, as it could happen that a component of the GM model fit on the data is actually representative of a correct coupling (rejection of meaningful data). To overcome this problem, it is possible to estimate the variation of the modal datum as relative to the variation of the mechanical parameter (i.e., if a mechanical parameter varies little, the direct consequence is that the modal datum will also have a limited variation).

$$\boldsymbol{\alpha_{n,kj}} = \frac{\boldsymbol{\alpha_{f,k}}}{\boldsymbol{\alpha_{p,j}}} \tag{6}$$

In Eq. (6), $\alpha_{f,k}$, $\alpha_{p,j}$, and $\alpha_{n,kj}$ are the variation indicator assumed for natural frequency, mechanical parameter, and normalized value, respectively. By normalizing the variation of the modal datum to that of the mechanical parameter (also estimated with the procedure previously described using GM models), it is possible to obtain an estimate of the variation not affected by the domain of variation of the mechanical parameter, which must in any case be a domain that respect the following conditions:

- composed of a large number of samples in order to reach a statistical significance also after the rejection of some data associated with misclassification errors;
- close to the correct values assumed by the parameter (e.g., knowledge of the experimental data or an estimate from literature).

The obtained variation, in the present work, estimated as the ratio between the coefficients of variation of the natural frequency and the mechanical parameter (i.e., Young's modulus, Poisson ratio, and density), can then be corrected by remultiplying its value by the real variation assumed by the mechanical parameters in different applications (e.g., model updating).

3. Application

To demonstrate the proposed methods, the FE model and the structure of Pavilion V of the Turin Exhibition Center are assumed as reference benchmark.

3.1. The structural system

The case under analysis is an underground building (also known as Pavilion V) designed by Riccardo Morandi in 1958 to expand the Exhibition Center, a complex dedicated to hosting large exhibitions events in the city of Turin. The structural scheme adopted by Morandi for Pavilion V is the so-called balanced beam in prestressed reinforced concrete, widely used by the designer between the 1950s and 1960s in bridges and overpasses [40].

The pavilion consists of a single large space, 69 m in width and 151 m in length, located 8 m below ground level. The structural scheme is composed of post-tensioned beams on two inclined supports, with two cantilevering side spans subsequently anchored by post-tensioning tendons at their ends, exerting a balancing effect on the bending moments in the main span. Unlike the usual bridge scheme, in Pavilion V, the main post-tensioned ribs are not parallel beams but are diagonally directed (see Fig. 1), but are diagonally directed and reciprocally interconnected in order to obtain a spatial structure offering high overall rigidity and lateral stability and to contrast the instability of the very thin beams (16 cm).

When dealing with heritage structures, it is crucial to consider that they often do not fully match what was conceived during the design phase and are reported in the technical drawings since changes were frequently encountered during the construction phase. This represents an important source of discrepancy that can affect the estimate of

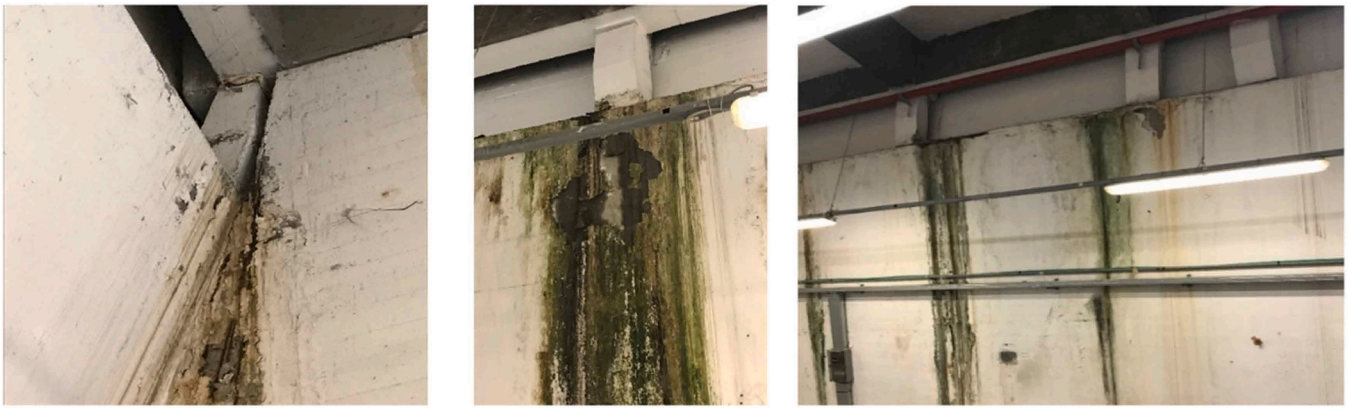

Fig. 2. Deterioration phenomena in connecting rods and perimetral walls of Pavilion V: the presence of efflorescence with a detachment of the concrete cover and corrosion of the reinforcement in the proximity of the joint (left) and at the central part of the blocks (center and right) [42].

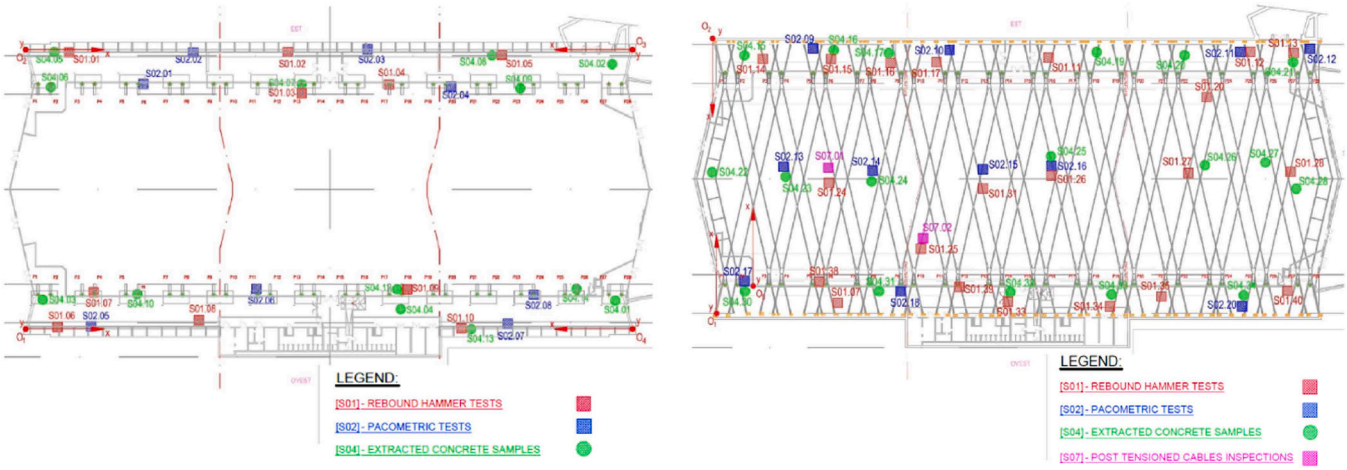

Fig. 3. Pavilion V: positions of the test setup at the underground floor (left) and at the roof level (right) [42].

sensitivity indicators and, consequently, the design of monitoring and conservation activities. For this reason, the numerical model used to optimize these activities should be initialized with information coming from preliminary experimental tests. A complete description of the Pavilion can also be found in [41].

3.2. The experimental mechanical tests

The experimental tests were aimed to reduce the uncertainty related to the geometry, structural details, and degradation state of the materials (see Fig. 2 and Fig. 3). In detail, inspections on the structure were carried out to determine: (i) the global discrepancy from the expected design situation, and (ii) the performance of materials. For this purpose, mechanical tests were executed to evaluate the compressive strength of the different elements of the structure.

Samples were extracted from foundations, perimetral walls, roof beams, and inclined struts. Then, the values of compressive strength were used to estimate the Young's moduli of the different structural components. In this sense, the tests were useful to initialize the virtual model of the structure and, in particular, the nominal value of the mechanical parameters. To this aim, the results of an additional test regarding the deflection of the roof beams were also used [42]. For more information about the experimental in-situ campaign carried out on the structure, the reader can refer to [43].

3.3. The virtual model

The FE model of the Pavilion is an excellent example for applying the methods proposed in this paper since its structure consists of a spatial architecture [44–46]. From a modal point of view, it is characterized by innumerable vibration modes in the vertical direction, many of which present a high number of inflections in the mode shape. This large number of inflections (i.e., *bubbles* modes) can generate a misclassification error because, during a simulated OMA, the eigenvectors are estimated on a small number of DoFs for computational reasons. The observation of the eigenvectors on a reduced domain can lead to the highest MAC between a reference mode and a set of vibration modes extracted from a numerical model being related to a mode not comparable with the reference one. In addition, the Pavilion consists of a jointed three-block structure. The three blocks are thus weakly connected through a perimeter wall linked by connecting rods to the roof beams. In such a situation, the modal behavior that most interests one block could easily be misinterpreted with that of another.

Finally, the Pavilion presents vertical and horizontal components of the mode shapes rather coupled, especially for the first vibration modes. This increases the possibility of error in the classification of the modal behavior when it is observed on a small number of DoFs (e.g., a local out-of-plane deformation of the roof slab characterized by horizontal movement could be erroneously interpreted for a diaphragmatic behavior of the same roof in the horizontal direction). The FE model is composed of eight structural components. In the linear elastic field, it contemplates just three material parameters for each component n, i.e.,

Table 1
Values of the elastic moduli after the corroboration phase.

Element	*Elastic moduli updated (Pa)*
Roof slab	39.9e9
Connecting rods and perimetral beams	33.0e9
Infill walls	2.12e9
Top and bottom edges of inclined struts	210e9

Young's modulus E_n, Poisson ratio ν_n, and density ρ_n. Initially, densities were assumed to be 2500 kg/m^3, excluding the expansion joints with zero mass and walls in cellular concrete with a density of 400 kg/m^3. Poisson's ratios were defined as equal to 0.2. The Young's moduli were defined starting from the mechanical tests described above.

It is worth to underling that the values used in the modelling refer to the static secant value obtained by tests, when available. This value is commonly slightly less than the dynamic value, which is needed during a modal based model updating. Indeed, the value of the Young's modulus is sensitive to static or dynamic loading [47]. However, since this work does not focus on automatic model calibration, and because the discretization of the reality generally leads to a numeric stiffening and overestimate of the natural frequency values, the choice to maintain the secant value of the Young's modulus leads to a compensation of the increase in stiffness due to the numerical discretization. During an automatic calibration phase instead, which goes beyond the scope of this work, the elastic moduli can be chosen and calibrated for the best representation of the modal behavior.

In particular, the values for roof beams, perimetral walls, and inclined struts are reported below. Since the external roof beams suffered torsional deformations starting from the conceptualization of the system, two box additional edge beams were provided to the structural system. The elastic properties of these elements were initialized as done for the roof beams and are reported hereinafter:

- Roof beams: 33e9 Pa
- Perimetral walls: 37e9 Pa
- Inclined struts: 32e9 Pa
- Edge beams: 33e9 Pa

Previous studies [41] showed that the stiffness of the joints can be considered zero, validating the initial hypothesis that joints between the diaphragms are working properly in operational conditions. In this situation, the three blocks are weakly connected just through the inner infill walls. For this reason, the expansion joints were omitted in conceptualizing the present virtual model since they would be associated to zero stiffness and mass. Instead, the deflection tests contributed to updating the roof model. Indeed, the density and Young's modulus of the roof were adjusted in the FE model to fit vertical displacements gathered during deflection tests. In particular, an increment of the density from 2500 kg/m^3 to 3500 kg/m^3 has been applied for the roof slab (with thickness variable between 25 cm and 45 cm) to simulate the permanent load acting on it as an overlying distributed mass. Whereas the Young's modulus has been increased from the initial reference value of 25e9 Pa to 39.9e9 Pa to simulate the equivalent stiffness of the roof, considering the layers positioned over the concrete slab: the concrete screed and the cement-stabilized soil. Instead, for the connecting rods and perimetral beams, the Young's modulus was initially imposed by literature; then, given the aging conditions in common with the roof beams, the value was modified by the experimental value obtained for those elements, i.e., 33e9 Pa. A typical Young's modulus, i.e., 3e9 Pa, has been initially assumed, according to the *SIA266* regulations, for the non-structural infill walls made of cellular concrete. Then, its value was modified after preliminary initialization of the model to match the first identified vibration mode in terms of mode shape and natural frequency [41]. The resulting value for this parameter is 2.12e9 Pa. Table 1 reports the values of the parameters for which no data were available from mechanical tests (roof slab, connecting rods and perimetral beams, and infill walls). The inclined struts are also provided with top and bottom edges made of steel in order to bear local stress concentration phenomena. The density of these elements is set to 7850 kg/m^3, while the Young's modulus is reported in Table 1.

As regards the FE characteristics, the model contemplates both 4-nodes shell and 2-nodes beam finite elements with six DoFs at each node (translation and rotations), which consider the shear deformability and maintain a linear law for the shape functions. The beam elements are used to model the curb positioned at the top of the perimetral walls, and the edges of the inclined struts. Instead, the shell elements are used to model the remaining part of the structure. The FE model counts approximately 27′000 elements for a total number of 165′000 DoFs and an average mesh size of 1.5 m. The model is fully restrained at the base; thus, mechanical foundation properties are not contemplated in this virtualization. The structural elements are then supposed internally fully restrained from each other. The three blocks that make up the structure are disconnected on the roof plane, while a slight connection is provided by the infill walls in cellular concrete. Finally, the model contemplates eight main structural components. For the analysis (eigen-analysis) only the self-weight of the structure is initially considered in the definition of the mass matrix. Fig. 4 reports the FE model of the Pavilion with components highlighted in different colors, while Table 2 reports the description of the components.

The first (first transverse mode #5 at 2.40 Hz) and last (first torsional mode #23 at 5.41 Hz) reference vibration modes used for the analysis are instead reported in Fig. 5 in terms of mode shapes. In addition, the analysis also contemplated the first #6 and second #7 vertical vibration modes of the slab at 2.62 Hz and 2.75 Hz, respectively, and the first

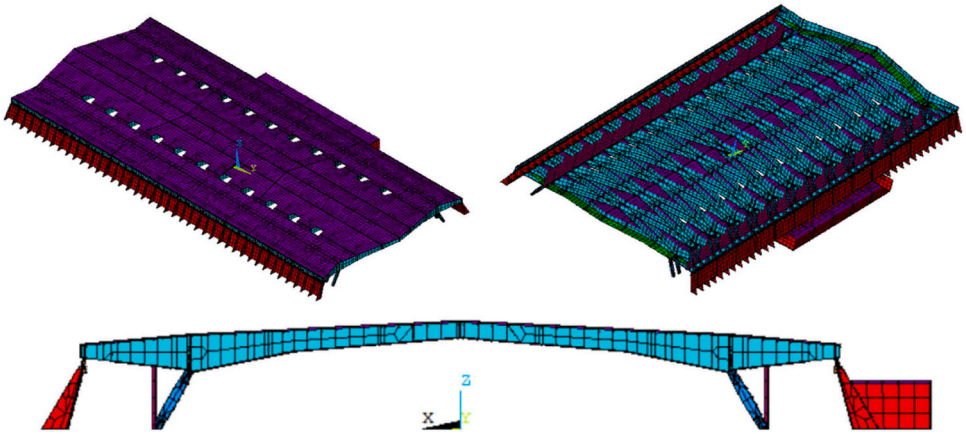

Fig. 4. Finite Element (FE) model of Morandi's Pavilion V (top, bottom, and front view).

Table 2
Description of the components of the Pavilion's numerical model.

FE component, n	*Description (material)*	*Representation*
1	Roof beams (prestressed concrete)	
2	Roof slab (reinforced concrete)	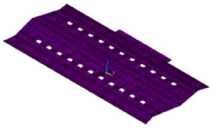
3	Perimetral walls (reinforced concrete)	
4	Inclined struts (reinforced concrete)	
5	Infill walls (cellular concrete)	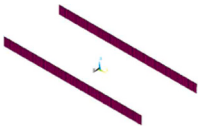
6	Edge beams (reinforced concrete)	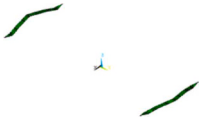
7	Connecting rods and perimetral beams (reinforced concrete)	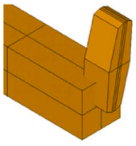
8	Top and bottom edges of inclined struts (steel)	

longitudinal mode #21 at 5.02 Hz. These are the main vibration modes of the center block of the Pavilion, which are used as benchmark for the analysis; however, the structure is composed of innumerable vibration modes that locally activate part of the system, or the remaining blocks. Vibration mode #1, for example, is the main transverse vibration mode of the left block, with torsional components on the right blocks. Vibration mode #2 activates the left edge beams of the right block in vertical direction. Vibration mode #4, instead, represents the main transverse mode of the right block of the Pavilion, with torsional components on the left block. Vibration mode #22 activates the edge blocks of the pavilion longitudinally, in counterphase, then, vibration mode #33 activates the vertical movement of the center block, with a flexural mode shape of the second type in the transverse direction and of the third type in the longitudinal direction, when compared to the vibrational modes of a simply supported beam. The natural frequencies and the associated mode shapes are reported in Fig. 5.

4. Results and discussions

In this section, the results of the analyses are reported and commented on. Fig. 6 reports the tracking of the mode number in the FE model for reference mode #5 as a function of the Young's modulus of infill walls.

While the modulus remains lower than 2.65e9 Pa, the coupling is quite correct and contemplates two classes. Between these two classes, a misclassification error appears. The same behavior can be perceived in Fig. 7, where the behavior of both natural frequency and MAC of the first transverse mode #5 is depicted as a function of the Young's modulus of the infill walls. It is quite easy to understand that misclassification errors can have a different nature: instantaneous-localized errors at 1.30e9 Pa, approximately, and continuous errors starting from 2.65e9 Pa, approximately. In this work, the first error is rejected with HHT, while the second error, is rejected with GM models fitted to natural frequency. The reader, however, can understand that meaningful information is erroneously also rejected (class associated to parameter values lower than 1.30e9 Pa). The algorithm mitigates this error by normalizing the natural frequency variation to the variation of the parameter (estimated in the center class, defined between 1.35e9 Pa and 2.65e9 Pa).

Fig. 8 reports the same concepts already described in Fig. 7, but in this case, the natural frequency and MAC of the first transverse mode #5 are depicted as a function of the Young's modulus of the roof beams. Fig. 9, instead, introduces a new concept. Here, the HHT of the MAC function reported in Fig. 8 is reported.

For convenience, the HHT domain has been normalized between zero and one. For this purpose, the following normalizations have been assumed:

$$l_n = 2\Delta p l \tag{7}$$

$$p_n = \frac{p - p_{\min}}{p_{\max} - p_{\min}} \tag{8}$$

where in Eq. (7) and Eq. (8) $p_{\min}$, $p_{\max}$, and Δp are the minimum, maximum and step size value of the sampled parameter assumed for the analysis (i.e., Young's modulus), while l_n and p_n are the normalized rate and normalized parameter axes.

It is possible to see that, contrary to Fig. 8, in Fig. 9, the outliers around 26e9 Pa (around 0.3 in the normalized space obtained using the stochastic oscillator indicator rule [48] applied to the parameter domain, see Eq. (8)) are well classified at high parameter rate (the threshold was manually calibrated and imposed at l_n=0.05 in this analysis). Thus, in this domain, it is quite easy to reject anomalies with respect to what may be done with the MAC function of the parameter: see, for instance, the outliers in Fig. 8 (values of parameter lower than 26e9 Pa) that take the same MAC values of correct classified vibration modes (values of parameter higher than 26e9 Pa).

Fig. 10 reports a fitting of the 2-variate distribution for the natural frequency of the first transverse mode #5 obtained by varying the Young's modulus of the roof beams. The correct component of the GM model to estimate the coefficient of variation of this modal parameter is the component with a lower MD to the reference value. In this case, the correct component is that on the right in Fig. 10.

After selecting the component with minimum MD from the reference natural frequency, its mean and standard deviation can be used to define a specific sensitivity indicator; in this case, it was assumed to use the coefficient of variation of the selected component v^*:

$$\alpha_f = \frac{\sqrt{\widehat{\Sigma}_{v^*}}}{|\widehat{\mu}_{v^*}|} \tag{9}$$

The coefficient of variation of the natural frequency α_f (see Eq. (9)) is then normalized to the coefficient of variation of the parameter α_p evaluated in the same class (same component) of the natural frequency to get the normalized coefficient of variation α_n. As needed, these

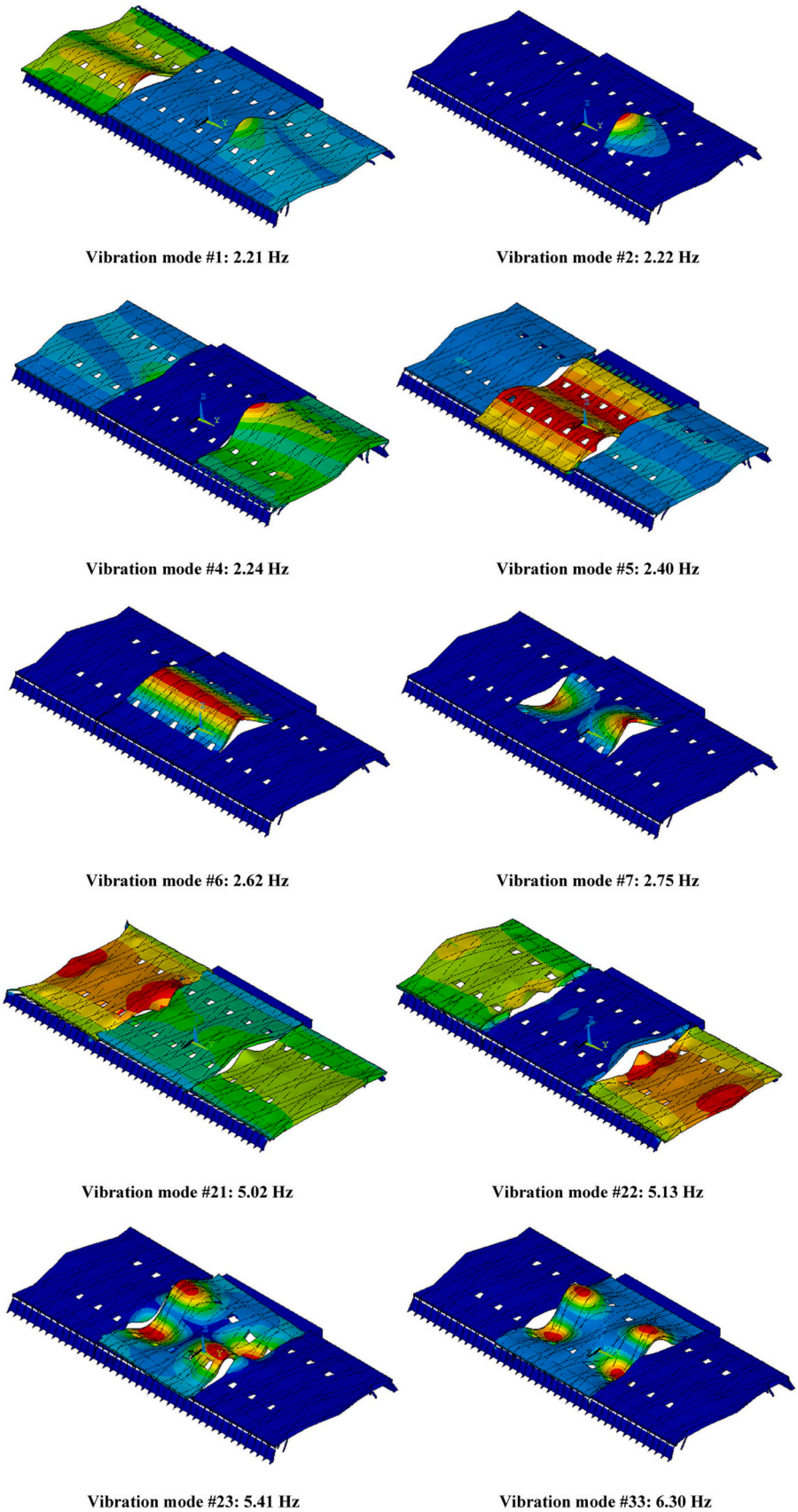

Fig. 5. Mode shapes of the main predicted vibration modes of the Pavilion.

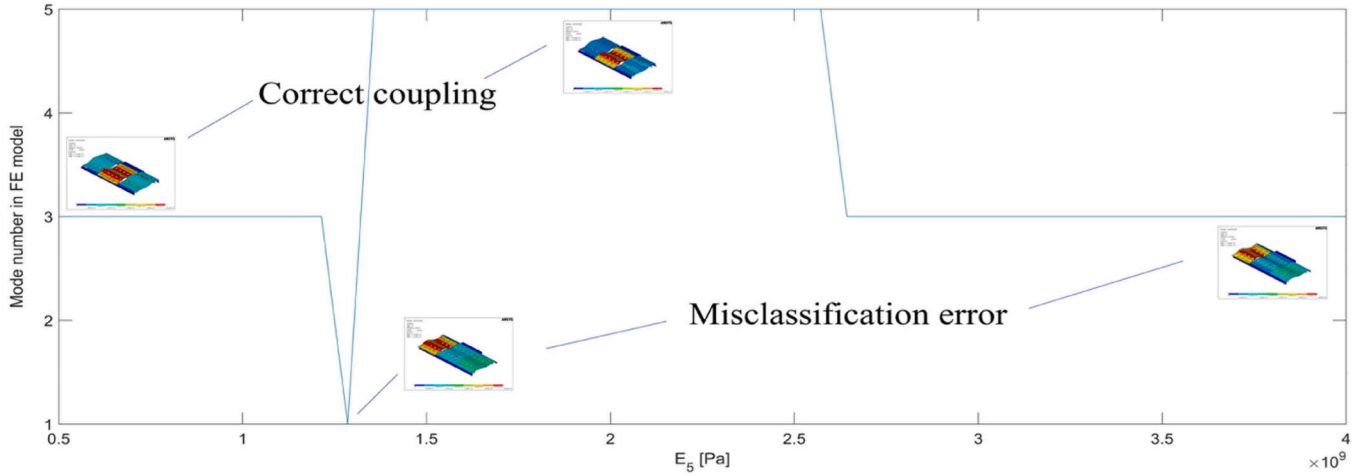

Fig. 6. Mode number in the FE model for the first transverse mode, as a function of the Young's modulus of the infill walls.

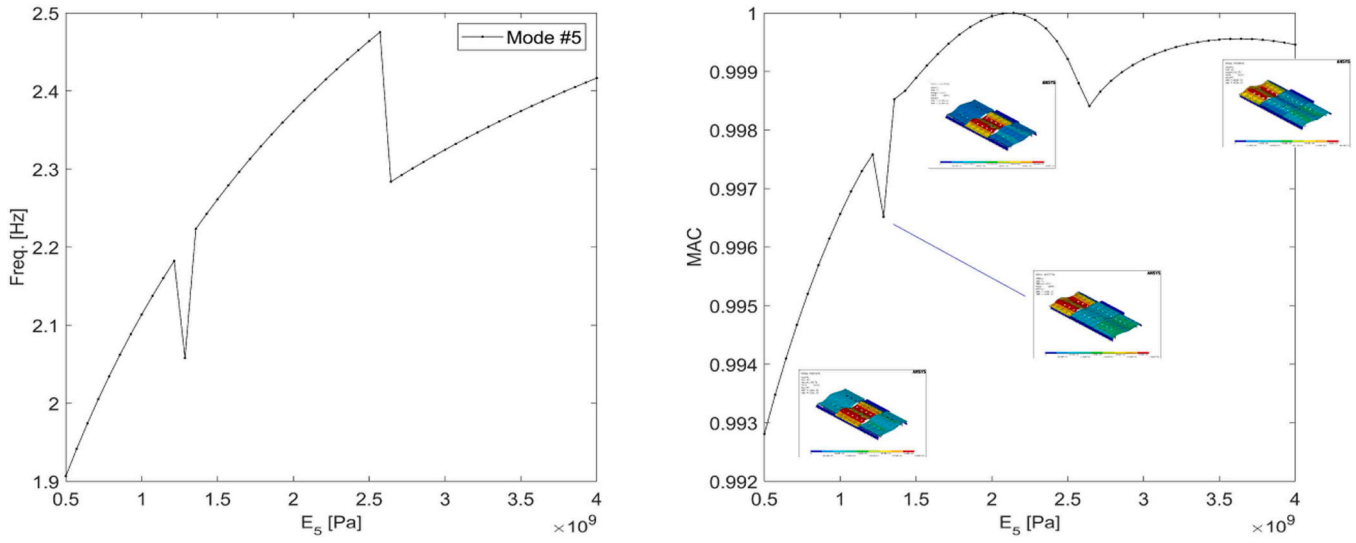

Fig. 7. Natural frequency and MAC of the first transverse mode, as a function of the Young's modulus of the infill walls.

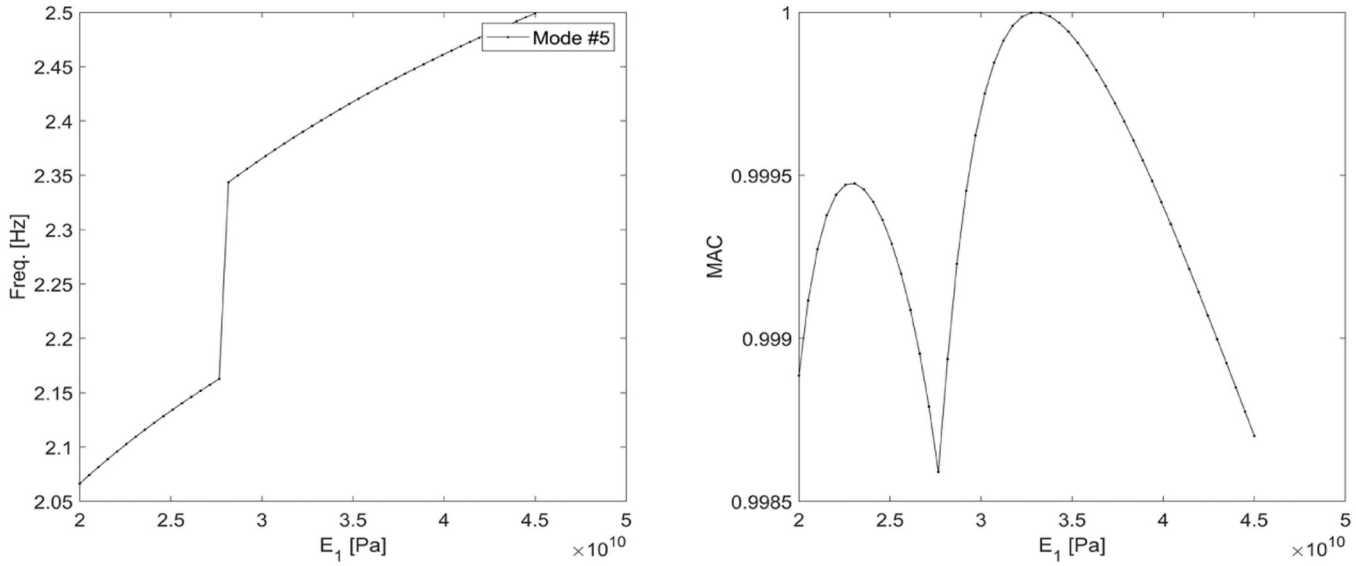

Fig. 8. Natural frequency and MAC of the first transverse mode, as a function of the Young's modulus of the roof beams.

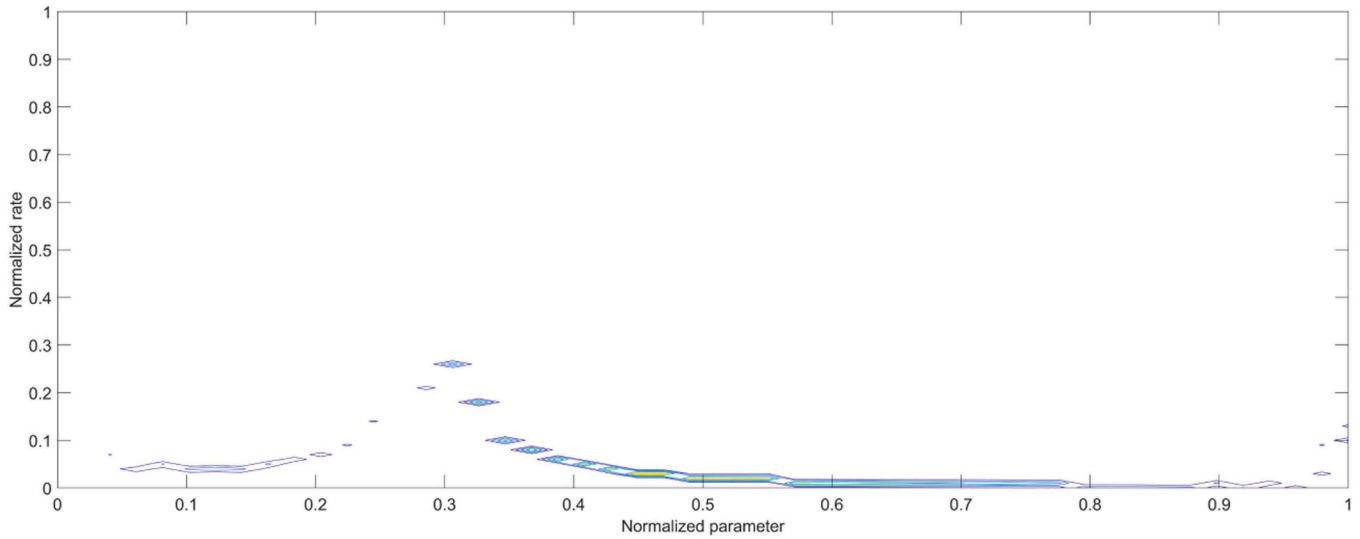

Fig. 9. Hilbert-Huang power spectrum as a function of the parameter rate (normalized to half of the sampling frequency of the parameter), and the normalized parameter value (normalized using the stochastic oscillator rule).

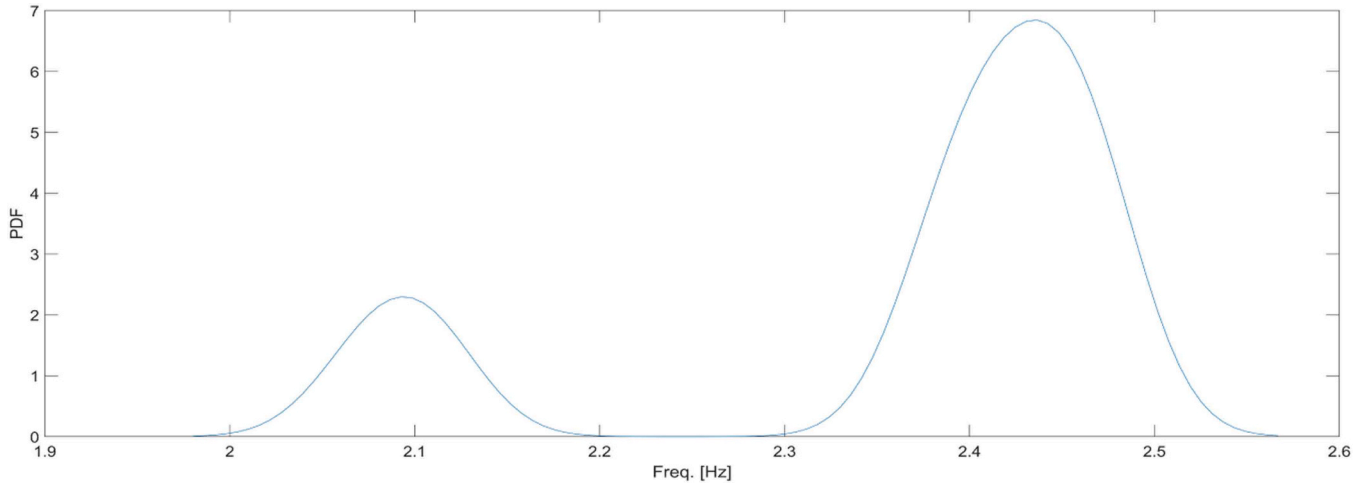

Fig. 10. Kernel estimate of the multivariate distribution (Probability Density Function - PDF) of the natural frequency of the first transverse mode (associated to the variation of the Young's modulus of the roof beams), after the misclassification error rejection.

relative variation estimators can be re-multiplied to the coefficient of variation of parameter values used for other purposes, such as the variation obtained by the parameter range used in model updating tasks (e.g., assuming a Gaussian prior distribution of the parameters). Fig. 11 reports these results in terms of normalized Fraction of Variation (FoV), that is, the variation estimators normalized to the sum of all contributions:

$$\boldsymbol{FoV}_{kj} = \frac{\boldsymbol{\alpha}_{n,kj}}{\sum_{k=1}^{K}\sum_{j=1}^{J}\boldsymbol{\alpha}_{n,kj}} \tag{10}$$

where in Eq. (10), K= 5 and J= 24 are the total number of vibration modes and mechanical parameters used in the sensitivity analysis. Table 3 reports the resulting ranking list of the first five mechanical parameters.

From the results of this study, it is possible to design monitoring systems and conservation operations in an optimized way. An example is the optimal experimental design of a permanent dynamic monitoring system. For instance, modal parameters are known to be influenced by Environmental and Operational Variations (EOVs), and their fluctuations produce physiological changes in modal behavior, which can hide more serious pathologies.

In this context, instrumenting area aimed at producing a greater variation of the modal behavior, for example, with thermometers applied on the most sensitive components (e.g., roof beams), or sensors capable of directly monitoring the variation of the mechanical parameters responsible for the majority of the variation of the modal parameters (e.g., load cell and strain gauges applied to the roof beams to records Young's modulus variations) can lead to the calibration of more truthful virtual models, capable of better capturing how EOVs influence modal data, and able to predict this trend for different purposes, such as structural monitoring and subsequent conservation.

5. Conclusions

Channeling resources in an optimized way helps to increase the knowledge level of a structure and, consequently, the reliability and accuracy of predictive analyses. Sensitivity analysis is a fundamental tool to achieve such optimization; however, its implementation encounters issues that should be addressed in order to obtain non-misleading results. In general, the errors that can be encountered

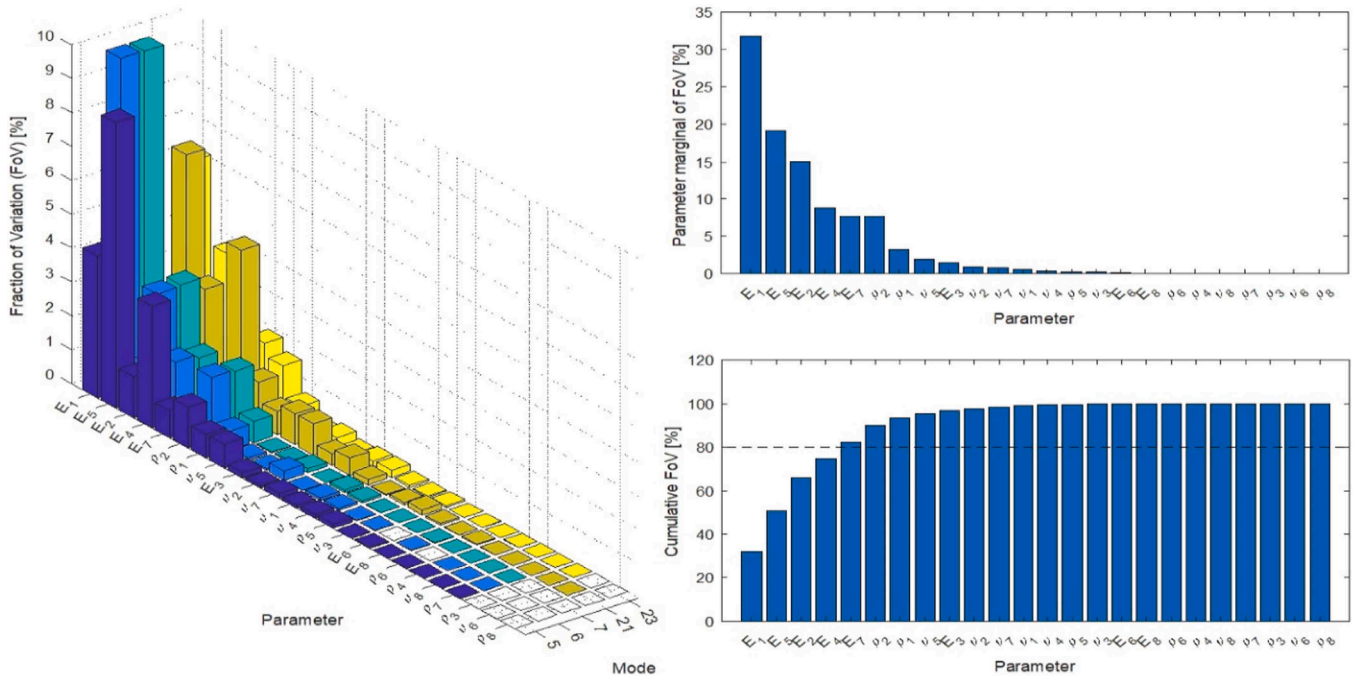

Fig. 11. Result of the sensitivity analysis in terms of the normalized Fraction of Variation (FoV) attributed to each parameter and each mode. On the top right, the marginal over the mode dimension is depicted, while on the bottom right, the cumulative sum of the marginal is reported. The achievement of 80 % of the total variation is highlighted with a dashed black line in the cumulative FoV plot.

Table 3
Ranking list of the main mechanical parameters responsible for at least 80 % of the total variation of the reference modal contributions (mode #5, #6, #7, #21, and #23).

FE component, n	*Mechanical parameter - component*	*Representation*
1	Young's modulus - Roof beams	
5	Young's modulus - Infill walls	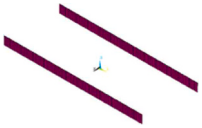
2	Young's modulus - Roof slab	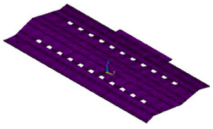
4	Young's modulus - Inclined struts	
7	Young's modulus - Connecting rods and perimetral beams	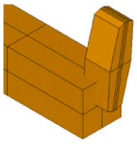

during the sensitivity indicator estimates could be of three types: (i) systematic error due to a poor initialization of the virtual model; (ii) localized misclassification errors; (iii) continuous or widespread classification errors. More in detail, during mode coupling (in sensitivity analysis based on modal data), vibration modes with high MAC value can be incorrectly associated to a target-controlled mode. In this context, the *correct* mode to be coupled to the reference one is characterized by a lower MAC value than the mode with the highest MAC. This problem is very common in architectural spatial structures where vertical and horizontal components of mode shape interact, especially in the presence of mode shapes characterized by a huge number of local *bubbles*, or even worse in the presence of interacting diaphragms, as in the case of Morandi's Pavilion V of Turin Exhibition Center. The method proposed in this paper mitigates these misclassification errors through the combined use of analogies with "time-frequency" analysis and Gaussian mixture models. The authors showed that:

- a variation of natural frequency contemplates the presence of a *true* variance, generated by the variation of the mechanical parameter, and a *false* variance component, generated by the misclassification (i.e., coupling error);
- very fast variations of MAC and natural frequency studied as a function of the assumed variation of mechanical parameters are associated with localized misclassification errors during the mode coupling process;
- these fast variations tend to be located at high parameter-rate values in the Hilbert-Huang space. This combined to the sparse nature of the Hilbert-Huang power spectrum, allows easy identification of the parameter values associated with the misclassification error, allowing error rejection in the calculation of the variance of the natural frequency.

Instead, for the errors due to poor initialization of the virtual model, experimental campaigns should be prescribed in order to increase the initial knowledge of the nominal value of the geometrical and mechanical parameters to be attributed to the numerical model. Future works can contemplate adaptative thresholding in the Hilbert-Huang

space to reject noise components due to localized misclassification errors and distributed misclassification errors.

CRediT authorship contribution statement

Erica Lenticchia: Data curation, Investigation. **GAETANO MIRAGLIA:** Conceptualization, Data curation, Methodology, Validation, Writing – original draft, Writing – review & editing. **Rosario Ceravolo:** Funding acquisition, Investigation, Project administration, Supervision. **Linda Scussolini:** Visualization.

Declaration of Competing Interest

The authors declare that they have no known competing financial interests or personal relationships that could have appeared to influence the work reported in this paper.

Acknowledgements

The authors wish to thank the Materials and Structures testing lab (MASTRLAB) and in particular Dr. Antonino Quattrone for his contribution in the test activities, which were also developed thanks to the building and logistics office of the Politecnico di Torino (EDILOG), and in particular thanks to Arch. Gianpiero Biscant. The research study, instead, has been conducted within the activities of Hy-Learn Project.

References

[1] Boscato G, Russo S, Ceravolo R, Fragonara LZ. Global sensitivity-based model updating for heritage structures. Comput-Aided Civ Infrastruct Eng 2015;vol. 30 (8):620–35.
[2] Zhang D, Lin X, Dong Y, Yu X. Machine-Learning-Based uncertainty and sensitivity analysis of Reinforced-Concrete slabs subjected to fire. Structures 2023;vol. 53: 581–94. https://doi.org/10.1016/j.istruc.2023.04.030.
[3] Lenticchia E, Miraglia G, Quattrone A, Ceravolo R. Condition assessment of an early thin reinforced concrete vaulted system. Int J Archit Herit 2023;vol. 17(2): 343–61.
[4] Brehm M, Brehm M, Zabel V, Zabel V, Bucher C, Bucher C. An automatic mode pairing strategy using an enhanced modal assurance criterion based on modal strain energies. J Sound Vib 2010. https://doi.org/10.1016/j.jsv.2010.07.006.
[5] To WM, To WM, Ewins DJ, Ewins DJ. Non-linear sensitivity analysis of mechanical structures using modal data. null 1991. https://doi.org/10.1243/pime_proc_1991_205_092_02.
[6] du Bois JL, du Bois JL, Lieven NAJ, Lieven NAJ, Adhikari S, Adhikari S. On the role of modal coupling in model updating. null 2009.
[7] Ubertini F, Comanducci G, Cavalagli N, Pisello AL, Materazzi AL, Cotana F. Environmental effects on natural frequencies of the San Pietro bell tower in Perugia, Italy, and their removal for structural performance assessment. Mech Syst Signal Process 2017;vol. 82:307–22.
[8] Allemang RJ. The modal assurance criterion–twenty years of use and abuse. Sound Vib 2003;vol. 37(8):14–23.
[9] Huang M, Li X, Lei Y, Gu J. Structural damage identification based on modal frequency strain energy assurance criterion and flexibility using enhanced Moth-Flame optimization. Structures 2020;vol. 28:1119–36. https://doi.org/10.1016/j.istruc.2020.08.085.
[10] Lofrano E, Romeo F, Paolone A. A pseudo-modal structural damage index based on orthogonal empirical mode decomposition. Proc Inst Mech Eng C J Mech Eng Sci 2019;vol. 233(23–24):7545–64.
[11] W. Heylen and P. Sas, "Modal analysis theory and testing," 2006.
[12] Maia NMM, Silva JMM. Modal analysis identification techniques. Philos Trans R Soc Lond Ser A: Math, Phys Eng Sci 2001;vol. 359(1778):29–40.
[13] Ewins DJ. Modal testing: theory, practice and application. John Wiley & Sons; 2009.
[14] Allemang RJ, Brown DL. Correlation coefficient for modal vector analysis. Proc Int Modal Anal Conf Exhib 1982.
[15] Allemang RJ. The modal assurance criterion–twenty years of use and abuse. Sound Vib 2003;vol. 37(8):14–23.
[16] Morales CA. Comments on the MAC and the NCO, and a linear modal correlation coefficient. J Sound Vib 2005;vol. 282(1–2). https://doi.org/10.1016/j.jsv.2004.04.011.
[17] Lieven NAJ, Ewins DJ. Spatial correlation of mode shapes: the coordinate modal assurance criterion (COMAC). Proc 6th Int Modal Anal Conf (IMAC) 1988.
[18] Hunt DL. Application of an enhanced coordinate modal assurance criterion. 10th Int Modal Anal Conf 1992.
[19] Brehm M, Brehm M, Zabel V, Zabel V, Bucher C, Bucher C. An automatic mode pairing strategy using an enhanced modal assurance criterion based on modal strain energies. J Sound Vib 2010. https://doi.org/10.1016/j.jsv.2010.07.006.
[20] Capellari G, Capellari G, Chatzi E, Chatzi E, Mariani S, Mariani S. Cost¯benefit optimization of structural health monitoring sensor networks. Sensors 2018. https://doi.org/10.3929/ethz-b-000278733.
[21] Cohen L. Time-frequency analysis, vol. 778. Englewood Cliffs: Prentice Hall PTR; 1995.
[22] Komkov V, Choi KK, Haug EJ. Design sensitivity analysis of structural systems, vol. 177. Academic press; 1986.
[23] Geng Y, Xue S, Shen Z. Outlier Detection Based on Hilbert-Huang Transform. 2011 Int Conf Remote Sens, Environ Transp Eng 2011:3311–4.
[24] Lehmann R. 3σ-Rule for outlier detection from the viewpoint of geodetic adjustment. J Surv Eng 2013;vol. 139(4):157–65. https://doi.org/10.1061/(asce)su.1943-5428.0000112.
[25] Neild SA, McFadden PD, Williams MS. A review of time-frequency methods for structural vibration analysis. Eng Struct 2003;vol. 25(6):713–28.
[26] Feng Z, Liang M, Chu F. Recent advances in time–frequency analysis methods for machinery fault diagnosis: a review with application examples. Mech Syst Signal Process 2013;vol. 38(1):165–205.
[27] Mustafa S, Yoshida I, Sekiya H. An investigation of bridge influence line identification using time-domain and frequency-domain methods. Structures 2021; vol. 33:2061–5. https://doi.org/10.1016/j.istruc.2021.05.082.
[28] Cohen L. Time-frequency distributions-a review. Proc IEEE 1989;vol. 77(7): 941–81.
[29] Wang Z-C, Ren W-X, Chen G. Time–frequency analysis and applications in time-varying/nonlinear structural systems: a state-of-the-art review. Adv Struct Eng 2018;vol. 21(10):1562–84.
[30] Mustafa S, Yoshida I, Sekiya H. An investigation of bridge influence line identification using time-domain and frequency-domain methods. Structures 2021; vol. 33:2061–5. https://doi.org/10.1016/j.istruc.2021.05.082.
[31] Huang NE, et al. The empirical mode decomposition and the Hilbert spectrum for nonlinear and non-stationary time series analysis. Proc R Soc Lond Ser A: Math, Phys Eng Sci 1998;vol. 454(1971):903–95.
[32] Looney D, Mandic DP. 13 - Empirical mode decomposition for simultaneous image enhancement and fusion. In: Stathaki T, editor. in *Image Fusion*. Oxford: Academic Press; 2008. p. 327–41. https://doi.org/10.1016/B978-0-12-372529-5.00008-1.
[33] Wu Z. Hilbert–Huang Transform and Its Applications. World Scientific; 2005.
[34] Huang NE, Wu Z, Long SR, Arnold KC, Chen X, Blank K. On instantaneous frequency. Adv Adapt Data Anal 2009;vol. 1(02):177–229.
[35] Borman S. The expectation maximization algorithm-a short tutorial. Submitt Publ 2004;vol. 41.
[36] G. McLachlan, "Peel., d," Finite Mixture Models, 2000.
[37] Civera M, Sibille L, Fragonara LZ, Ceravolo R. A dbscan-based automated operational modal analysis algorithm for bridge monitoring. Measurement 2023: 112451.
[38] Sun Q, Rainieri C, Ren WX, Yan WJ, Fabbrocino G. Automated operational modal analysis of bell towers subjected to narrowband input. Structures 2023;vol. 54: 78–88. https://doi.org/10.1016/j.istruc.2023.05.034.
[39] De Maesschalck R, Jouan-Rimbaud D, Massart DL. The mahalanobis distance. Chemom Intell Lab Syst 2000;vol. 50(1):1–18.
[40] Levi F, Chiorino MA. Concrete in Italy. A review of a century of concrete progress in Italy, Part 1: Technique and architecture. Concr Int 2004;vol. 26:55–61.
[41] Ceravolo R, Lenticchia E, Miraglia G, Oliva V, Scussolini L. Modal identification of structures with interacting diaphragms. Appl Sci 2022;vol. 12(8):4030.
[42] Diseg M. Prove di caratterizzazione meccanica dei materiali e prove di carico sulla struttura di copertura del Padiglione V Torino Esposizioni. Intern Tech Rep 2019.
[43] Ceravolo R, Lenticchia E, Miraglia G, Oliva V. Degradation of structural safety levels in prototype balanced beam systems. Structures 2024:106434.
[44] Scheder-Bieschin L, Bodea S, Popescu M, Van Mele T, Block P. A bending-active gridshell as falsework and integrated reinforcement for a ribbed concrete shell with textile shuttering: Design, engineering, and construction of KnitNervi. Structures 2023;vol. 57:105058. https://doi.org/10.1016/j.istruc.2023.105058.
[45] Lenticchia E, Ceravolo R, Chiorino C. Damage scenario-driven strategies for the seismic monitoring of XX century spatial structures with application to Pier Luigi Nervi's Turin Exhibition Centre. Eng Struct 2017;vol. 137:256–67.
[46] Lenticchia E, Ceravolo R, Antonaci P. Sensor placement strategies for the seismic monitoring of complex vaulted structures of the modern architectural heritage (vol) Shock Vib 2018;2018. https://doi.org/10.1155/2018/3739690.
[47] Chisari C, Bedon C, Amadio C. Dynamic and static identification of base-isolated bridges using Genetic Algorithms. Eng Struct 2015;vol. 102. https://doi.org/10.1016/j.engstruct.2015.07.043.
[48] P.K. Romano, "Application of the stochastic oscillator to assess source convergence in Monte Carlo criticality calculations," 2009.